The sulfur-containing antibiotic BE-7585A: a study of its synthesis

By: David Donghyun Kim

In partial fulfillment of the requirements for graduation with the
Dean's Scholars Honor's Degree in Biochemistry

_____ _____

Dr. Hung-wen Liu — Date
Supervising Professor

_____ _____

Dr. John F. Stanton — Date
Honor's Advisor in Biochemistry

I grant the Dean's Scholars Honors Program to:

__X__ Post a copy of my thesis on the Dean's Scholars website

__X__ Keep a copy of my thesis in the Dean's Scholars office

The sulfur-containing antibiotic BE-7585A: a study of its synthesis

Department of Chemistry and Biochemistry
College of Pharmacy

_____
Name

_____ _____
Signature Date

_____ _____
Supervising Professor Date

_____
Signature

Table of Contents

Abstract

Antibiotics are often differentiated and divided using two classes, grouped by function and structure. The molecular basis and mechanism of action of many antibiotics have been studied and identified through recent advancements in molecular biology. The main structural feature of BE-7585A is an angucycline ring. Antibiotics with this unique ring structure are known to have diverse biological functions such as antitumor, enzyme inhibitory, and blood platelet aggregation inhibitory activity [1]. Although the biological effects of BE-7585A have not been studied in detail, similar synthetic pathways have begun to be elucidated, such as urdamycin and aquayamycin by the Rohr Group [2]. However, unlike urdamycin, BE-7585A has a unique feature. It is one of few *naturally* occurring compounds containing a C-2 thiosugar. The incorporation of this sulfur moiety in this compound, or any other C-2 thiosugar compounds, has never been studied. Two main experiments were carried out in this work to study and elucidate part of the biosynthetic pathway of this C-2 thiosugar formation. First, a pull-down assay was performed to find the sulfur donor critical to the pathway. Second, kinetic studies of the 2-thio-trehalose-6-phosphate synthase were done to determine the k_m and v_{max} values. Although the results of the first experiment were found to be inconclusive, the kinetic parameters of the reaction catalyzed by the 2-thio-trehalose-6-phosphate synthase were determined.

Introduction

The biosynthetic pathway of BE-7585A was proposed by graduate student Eita Sasaki. The focus of the experiments in this paper lies mainly within the final portions of the pathway, where the sulfur incorporation occurs. The pathway highlighting only this portion is shown below:

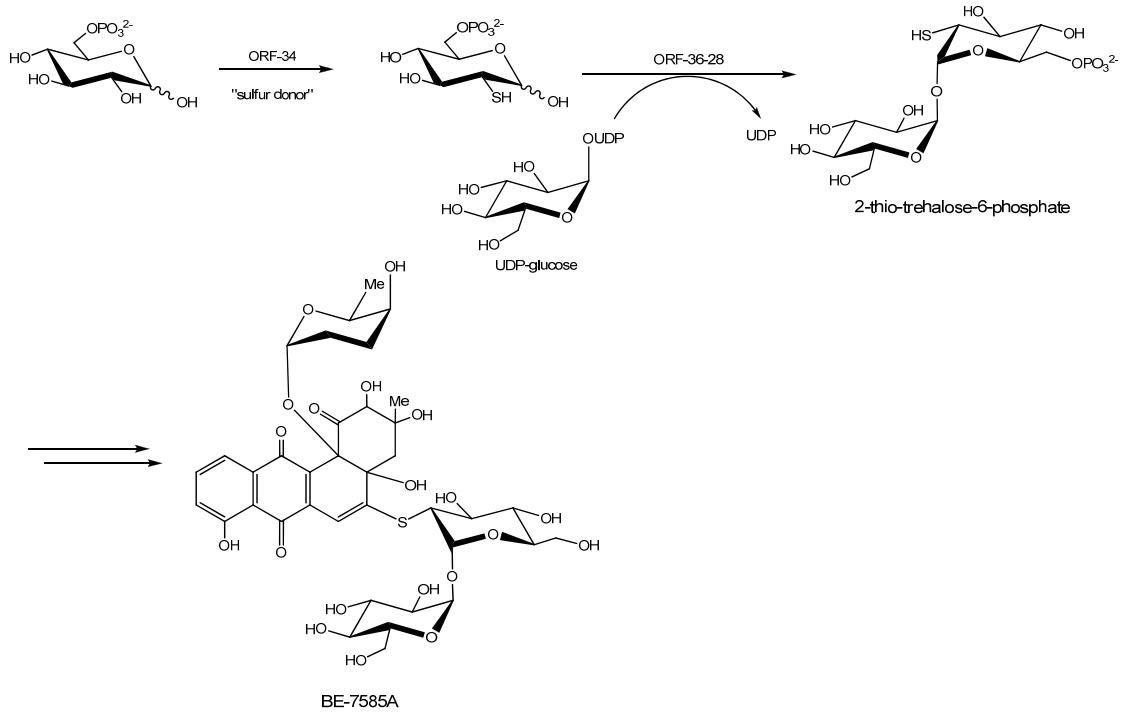

Figure 1: Sulfur incorporation pathway of BE-7585A

The angucycline ring and rhodinose biosynthesis pathways were also proposed by Eita. The rhodinosyl moiety is transferred to the angucycline ring portion via ORF-25 which has glycosyl transferase activity, much like the synthesis of urdamycin A [3]. However, the only experiment that I was involved in for this was purifying the ORF-25 enzyme through immobilized metal affinity chromatography (IMAC) using Ni-NTA resin.

The conversion of glucose-6-phosphate to 2-thio-glucose-6-phosphate in the first step (See *Figure 1*) is catalyzed by the enzyme ORF-34 (a thiazole synthase homologue), but requires the presence of a sulfur donor. Two candidates were considered: gluthathione (GSH)

and a ThiS-like protein. Gluthathione first was tested using a trapping experiment by Eita and was determined not to be the donor. The second possible sulfur donor in the mechanism for the 2-thiosugar formation is a ThiS-like protein. This gene homolog can be found the biosynthetic gene cluster. In order to identify the putative ThiS-like protein, a pull down assay was performed. A pull down assay is commonly used to determine whether a protein has a certain affinity to another [4]. ORF-34 expressed in *S. lividans* has a hexahistidine tag at the N-terminus (and C-terminus for ORF34-24) which preferentially binds to the Ni-NTA resin. In thiamine biosynthesis, the ThiS protein binds to ThiG [5]. This means that they can be copurified together. Because ORF-34 has a similar function as ThiG, it may be used as a bait to draw out the ThiS-like protein in this manner. The cell-free extracts from *A. orientalis vinearia* was carefully prepared that contained the contents of the cell, and hopefully, the ThiS-like protein. The pull down results can then be examined by running a SDS-PAGE.

The second step in the sulfur incorporation pathway is the formation of 2-thio-trehalose-6-phosphate. ORF-36, a trehalose phosphate synthase homolog, is proposed to catalyze the glycosyl transfer reaction between 2-thio-glucose-6-phosphate (2SG6P) and UDP-glucose (UDPG). Because of the importance of this reaction, kinetic analysis of the enzyme is important especially when comparing it to other trehalose phosphate synthases. However, the scarcity of 2SG6P and the difficulty in synthesizing the compound for experimentation is a barrier to the study. Luckily, ORF-36 can also catalyze the same reaction by replacing 2SG6P with an analogue, glucose-6-phosphate (G6P), to form trehalose-6-phosphate. This makes sense because in a biological system, both 2SG6P and G6P coexist. It was demonstrated in earlier experiments by Eita that ORF-36 preferentially uses 2SG6P over G6P, which confirms that ORF-36 is actually a 2-thio-trehalose-6-phosphate synthase. The scheme for measuring the rate of this enzyme is shown as *Figure 2*.

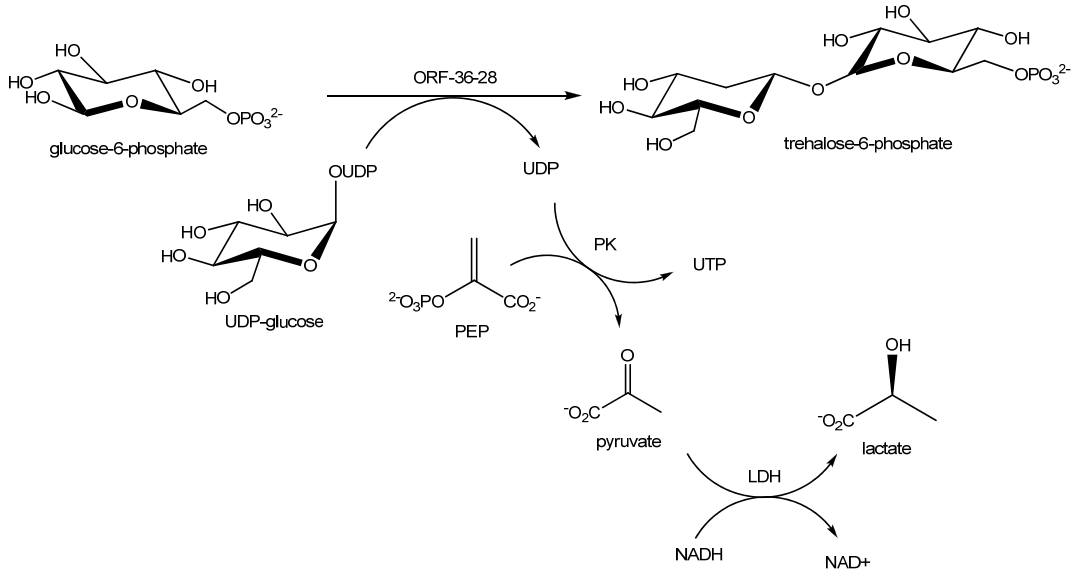

Figure 2: ORF-36 reaction using pyruvate kinase and lactate dehydrogenase detection.

A byproduct of the ORF-36 reaction is the formation of UDP from UDP-glucose. UDP is then converted to UTP by pyruvate kinase, which uses phosphoenolpyruvate (PEP) as a cosubstrate. The removal of a phosphate group from PEP forms pyruvate, which is then used by lactate dehydrogenase (LDH) to form lactate. The LDH reaction is the key part of the scheme because it consumes NADH, which is readily measureable spectroscopically.

The absorbance of 150 uM NADH at 340 nm is approximately 1. By measuring the reaction at 340 nm, the concentration of NADH can be monitored. Because 1 equivalent of G6P and UDPG is converted to the disaccharide product in the reaction scheme along with the concomitant transformation of 1 equivalent of NADH to NAD^+, the decrease in the concentration of NADH per minute can be used to determine the enzyme's kinetics. In this assay, the pyruvate kinase and lactate dehydrogenase reactions have to occur very fast in respect to the ORF-36 reaction in order for this scheme to work. A published journal article has confirmed the effectiveness of the PK/LDH assay with trehalose-phosphate synthase in *M. tuberculosis* [6]. A very powerful advantage of this reaction scheme is that it can be done in real-time (continuously).

A pH dependency study of ORF-36 was done by performing the reaction at different

pH ranging from 5.7 to 7.82 to determine the best conditions for the assay using G6P as the substrate. Next, the k_m/k_{max} values were measured at different concentrations for UDPG and G6P to get a rough estimate of the values for future experimentation with 2SG6P, and to optimize the assay system. The kinetic values can be determined graphically using two methods: the double reciprocal plot and the direct linear plot. Traditionally, kinetic values are estimated using the former. This is a plot with inverted substrate concentration and velocity as the *x* and *y* axes. The *x* and *y* intercepts of the regression lines give the values of $-\frac{1}{K_m}$ and $\frac{1}{V_{\max}}$, respectively. However, the direct linear plot has several advantages to the double reciprocal plot. It is very simple to construct and requires no modification of the data, and it also provides a quick view about the quality of the observations. Like the double-reciprocal plot, the direct linear plot only works for kinetic experiments in which the Michaelis-Menten equation is obeyed [7]. The common intersection point between the lines is the best estimate of k_m and v_{max}. Ideally, all lines would intersect at a single point (k_m, v_{max}). However, this is never the case experimentally. In fact, all regression lines must be assumed to intersect at different points, even if they appear otherwise. The total number of intersections is given by the equation:

$$\text{Total number of intersections} = \frac{1}{2}n(n-1) \qquad \textbf{(Eq 1)}$$

Thus, since there are 4 different concentrations of the substrate (UDPG), there are 6 intersections for each G6P concentration. The best estimates of k_m and v_{max} are then taken as the medians of each set.

Methods and Materials

Immobilized Metal Affinity Chromatography (IMAC) Protein Purification

Preparation, incubation, elution, and storage

1L of frozen overnight culture of *E. coli* cells were resuspended in 40 mL of lysis buffer (pH 8.0) containing 50 mM Tris-HCl, 300 mM NaCl, 10 mM imidazole, and 10% glycerol. Fresh lysozyme was added to the suspension with a final concentration of 1 mg/mL. This was incubated on ice for 30 min and sonicated on ice using Sonic Dismembrator 550. The total pulse time was 1 min and 40 sec, in 10 sec intervals with 30 sec rest time on full power. Aliquots of 10 µL of this whole cell mixture was saved for PAGE analysis. This was then centrifuged at 20,000×g for 20 min at 4°C. Again, 10 µL of the supernatant was saved for PAGE analysis. The supernatant was mixed with the Ni-NTA resin and incubated on the orbitron for 2 h at 4 °C. After incubation, the resin was left to settle for 20 min, and 10 µL of the supernatant (flowthrough) was taken for PAGE analysis. The mixture was poured into the column and washed with wash buffer containing 20 mM imidazole. Then the protein bound to the resin was eluted using elution buffer containing 250 mM imidazole, and collected in 1 mL fractions. From each fraction, 2 uL was mixed with 100 µL of Bradford reagent in an ELISA titer to analyze which fractions contained the target protein. PAGE samples were made for all fractions, and the fractions containing a significant amount of protein were transferred to a dialysis bag and dialyzed for 1 h in 1 L of dialysis buffer containing 50 mM Tris-HCl, 300 mM NaCl, and 15% glycerol with 3 changes. The protein were then split into 100 uL aliquots and flash frozen using liquid nitrogen and stored at -80 °C.

Pull Down Assay of ORF34-ThiS Complex

Preparation of cell-free extracts

The cell free extracts of *A. orientalis vinearia* were prepared using a modified version of a previously published protocol [8]. An extraction buffer was prepared that contained 50 mM potassium phosphate (pH 7.5), 30% glycerol, 2 mM mercaptoethanol, 0.1 mM phenylmethylsulfonyl fluoride, 0.1 mM benzamidine HCl, and 1 mM EDTA. A.O.V cells were resuspended into the buffer and pipetted into liquid nitrogen, forming frozen miniature balls. Using the Mixer Mill MM 300 at the ICMB Core Facility, the frozen cells were grinded into a fine powder, and resuspended in the extraction buffer. The crude cell free extracts were then centrifuged at 4,000×g for 20 minutes and the resulting supernatant was dialyzed in buffer containing 50 mM Tris-HCl, 300 mM NaCl, and 15% glycerol.

Incubation of ORF34 with cell free extract

In an Eppendorf tube, 25 µL of ORF-34, 50 µL of Ni-NTA resin, and 925 µL of cell free extracts (total 1 mL mixture) were added and incubated on the orbitron for 4 h. The mixture was then centrifuged and the supernatant was discarded. The resin was washed using wash buffer (20 mM imidazole), and the proteins were eluted using elution buffer (250 mM imidazole). The eluate were then analyzed with SDS-PAGE using 12% acrylamide, electrospray ionization mass spectrometry, and in-gel trypsin digestion. Four sets of reactions were done, as shown below in *Table 1*.

TABLE 1: Pull-down Assay reactions

	Cell Free Extracts	ORF34-24	ORF34-28	Ni-NTA resin	G6P (1mm final)
1	+	+	+	+	–
2	+	–	–	+	–
3	–	+	+	+	–
4	+	+	+	+	+
	(850 uL)	(25 uL)	(25 uL)	(100 uL)	(10 uL)

For the Western blot, conditions were slightly modified.

TABLE 2: Pull-down Assay reactions for Western blot

	Cell Free Extracts	ORF34-24	ORF34-28	Ni-NTA resin
1	+	+	–	+
2	+	–	+	+
3	–	+	–	+
4	–	–	+	+
5	+	–	–	+
	(580 uL)	(50 uL)	(50 uL)	(~100 uL)

Lastly, the conditions for the high-resolution gel was simplified.

TABLE 3: Pull-down assay for high-resolution gel

	ORF34-24	ORF34-28	Cell Free Extracts
1	+	–	+
2	–	+	+

Kinetic measurements of ORF-36

Preparation of enzyme

The ORF-36 protein was expressed in *E. coli* (BL-21*) and allowed to incubate for 3 days. The cells were harvested, and the enzyme was purified through a Ni-NTA column as previously described. The enzyme concentration was measured by Bradford assay to be approximately 31 mg mL^{-1}.

Preparation of reaction buffer and spectrophotometer settings

The reaction solution was made containing 0.2 ~ 20 mM G6P, 300 uM PEP, 150 uM NADH, 10 mM $MgCl_2$, and 50 mM Tris-HCl (pH 8.0). To 92 uL of the reaction buffer, 0.1 ~ 4 mM UDPG and 1 uL of PK/LDH enzyme were added for a total of 98 uL. Each reaction took place in a 100 uL UV cuvette. The Beckman-Coulter DU650 spectrophotometer was used on kinetics mode, measuring at 340 nm wavelength for 20 min runs at room temperature. After 2 min, 2 uL of ORF-36 was quickly added and mixed, and monitored.

Results and Discussion

Part I: Pull-down Assay of ThiS in *A. orientalis*

The ThiS protein in *B. subtilis* has a molecular weight of ~7.2 kD and the size of ORF34 is ~26.9 kD [9]. SDS PAGE analysis of the pull-down assay initially showed a small band smaller than 6.5 kD on lanes 1 and 4 which contained both ORF34 and the cell free extracts, and no bands on lanes 2 and 3 which was missing either ORF34 or the cell free extracts (refer to methods and materials for exact conditions). *Figure 3* shows the PAGE results dyed in Coomassie blue and silver stain.

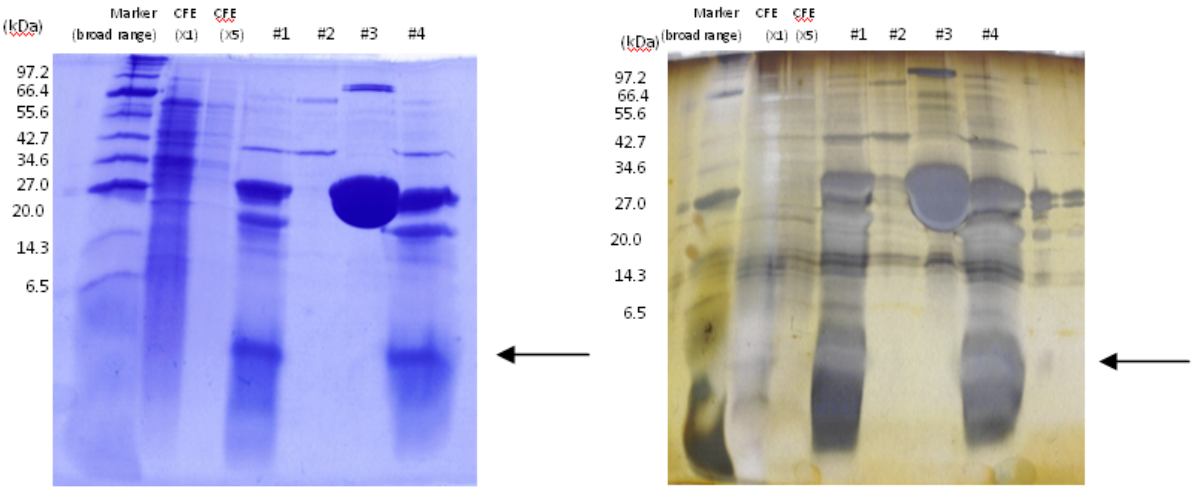

Figure 3: Coomassie and silver stain gels indicate the possibility of a ThiS-like protein in the pull down.

The results looked promising, so a Western blot of the gels of another pull down assay using the same conditions with time dependency were done. *Figure 4* shows the PAGE gel and the corresponding Western blot.

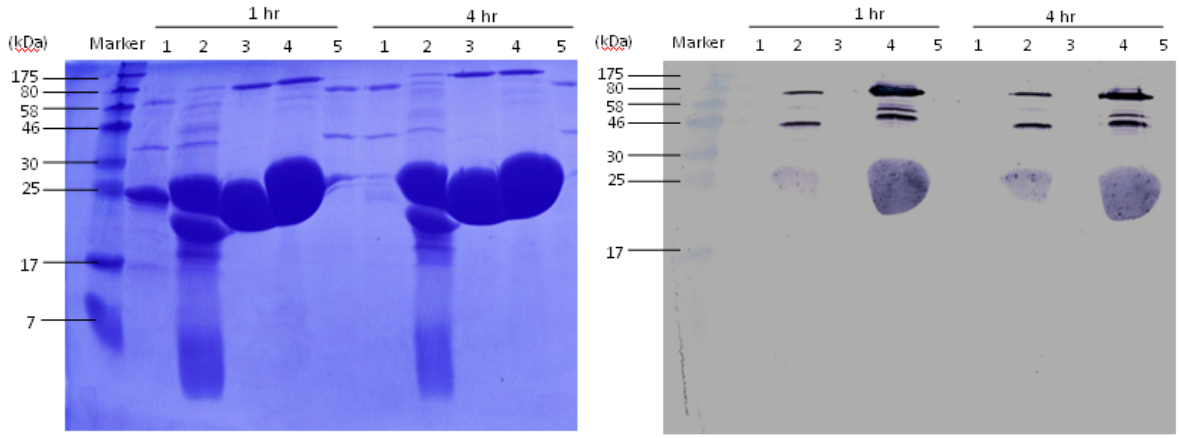

Figure 4: PAGE gel (left) and Anti-his Western blot (right) show that only lanes 2 and 4 contain actual protein.

Time dependency was not conclusive, but lanes 1-4 all should have had bands on the Western blot. However, only lanes 2 and 4 which contained only ORF34-28 showed bands. This means that the pull-down assays using only ORF34-24 probably had degraded protein. The original experiment shown in *Figure 3* had a protein mixture containing both ORF34-24 and ORF34-28, so we were unable to see this difference beforehand. To confirm again, another pull down assay was done and the eluents were run on a high resolution gradient PAGE as shown in *Figure 5*. Refer to *Table 3* for the conditions.

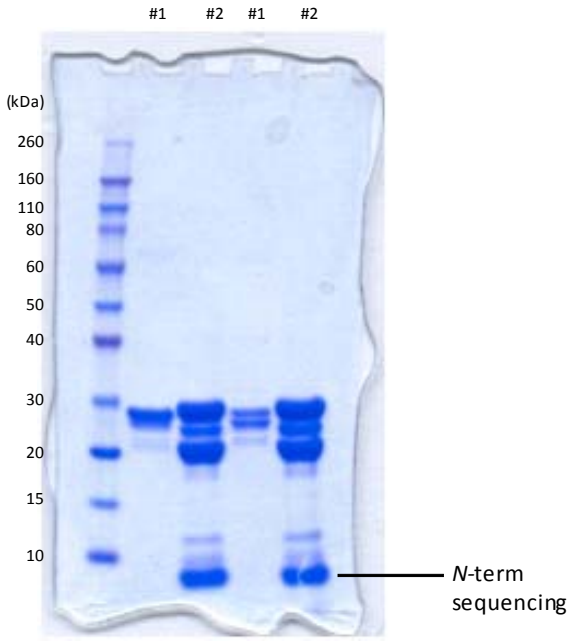

Figure 5: High-resolution gradient PAGE showing the fragment size and the band used for trypsin digestion.

This was then submitted for in-gel trypsin digestion for N-terminal amino acid sequencing. The result of the digestion showed that the N-terminal sequence of the protein was N-GSSHHHHHH. This proved that the small protein seen on the gel was a degraded fragment of the protein.

Usually, tags placed on the end of proteins for purification purposes has little to no effect on its function. An interesting conclusion of this experiment was that the placement of the hexahistidine tag is important for the stability of ORF34. The only difference between ORF34-24 and ORF34-28 is that the former has the tag placed on the C-terminus, whereas the latter has the tag on the N-terminus. For future studies, ORF34-28 should be used for its better stability.

The ThiS-like protein that we were aiming for was not obtained using this method. However, the genome of *A. orientalis* has been recently sequenced by the Genomics Research Center of Academia Sinica in Taiwan, so that the ThiS-like protein could be identified through genome mining.

Part II: Enzymatic studies of ORF36-28

The results of the pH dependency experiment show that the rate of NADH consumption increases at higher pH (7.82).

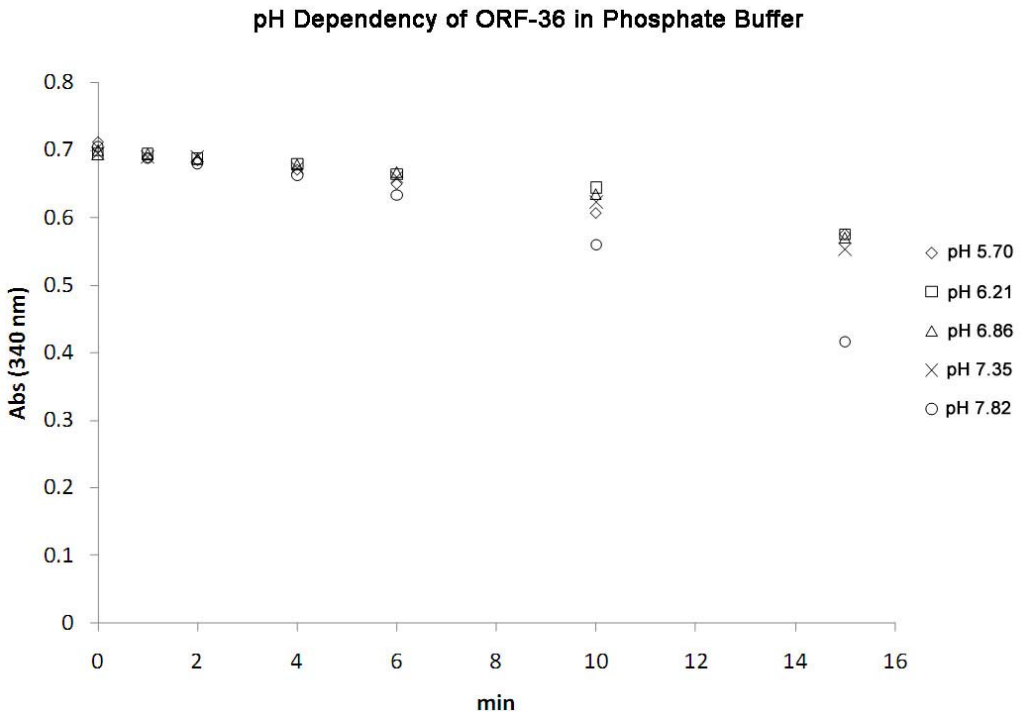

Figure 6: Absorption of NADH showing the activity of ORF-36 at various pH.

This means that the enzyme is more active at a higher pH. Although the buffer system used in this experiment was sodium phosphate (Tris has a different effective pH range), it is expected that the enzyme will behave similarly in Tris. Thus, subsequent experiments were carried out in pH 8 Tris buffer.

Two methods were used for determining the k_m and v_{max} for ORF-36. The first method was the Lineweaver-Burk (double-reciprocal) plot, which is a graphical representation of enzyme kinetics modeled by the Michaelis-Menten equation. *Figure 5* shows the double-reciprocal plot of 4 different concentrations of G6P at different concentrations of UDPG.

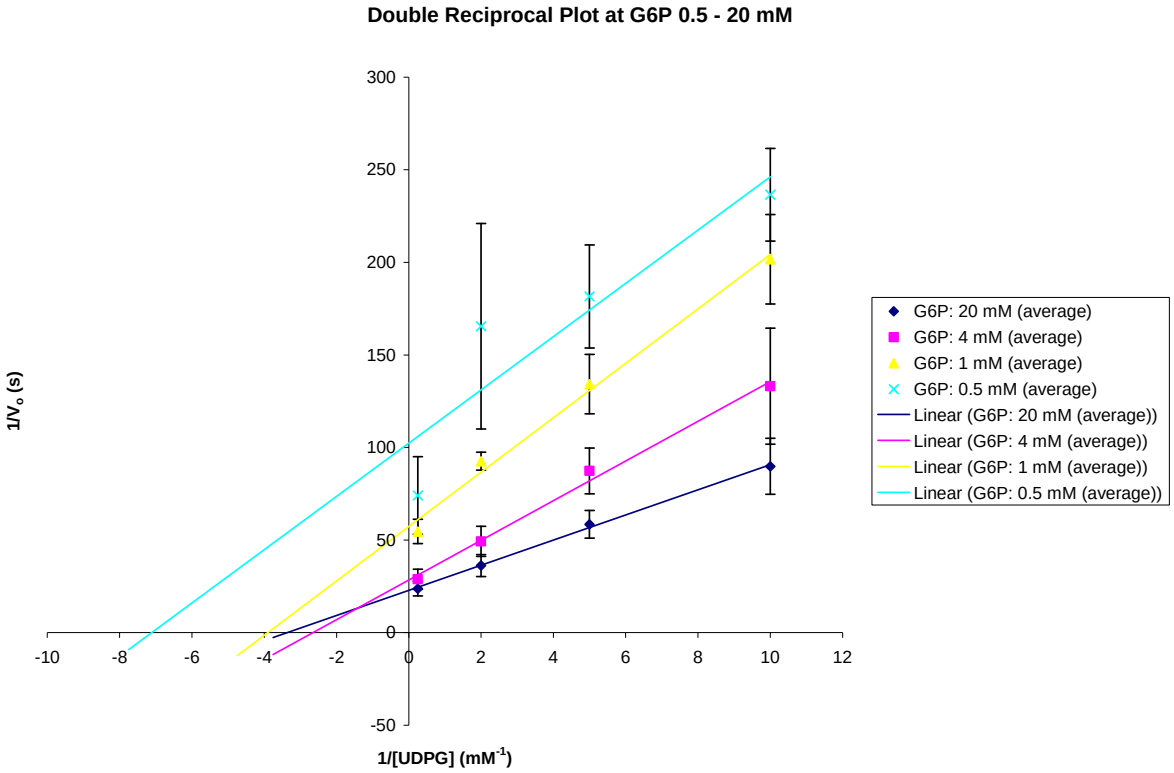

Figure 7: Lineweaver-Burk Plot of the ORF-36 coupled assay reaction

Each point on the graph is the average of 3 sets of runs with standard errors shown. As expected, the standard error on 0.5 mM G6P is the largest due to the reciprocal nature of the plot, as well as the uncertainty of the reaction at such low concentration. This is because the assay reaction needs time for intermediates to build up. Based on the data shown by the graph, however, there are two possible ways in which ORF-36 can proceed. First, the competitive inhibition pattern of the lines of 20 mM and 4 mM G6P show that ORF-36 can possibly act in a bi-bi sequential mechanism with UDPG binding first [10]. Secondly, the 1 mM and 0.5 mM G6P lines exhibit a "ping-pong" mechanism. It may be possible that ORF-36 reacts using both methods, depending on the concentration of the G6P substrate (and 2SG6P in cellular conditions). Future experiments should be done to confirm this hypothesis.

Table 4 summarizes the k_m and apparent v_{max} values of each G6P concentration using this method.

TABLE 4: K_m and V_{max} values determined using Double Reciprocal Plot

	Apparent K_m (mM)	Apparent V_{max} (s^{-1})
20 mM G6P	0.30	0.044
4 mM G6P	0.38	0.035
1 mM G6P	0.26	0.017
0.5 mM G6P	0.14	0.010

An alternative way to plot the data is the direct linear plot, developed by Athel Cornish-Bowden. The direct linear plot for ORF-36 for 20 mM G6P is shown below.

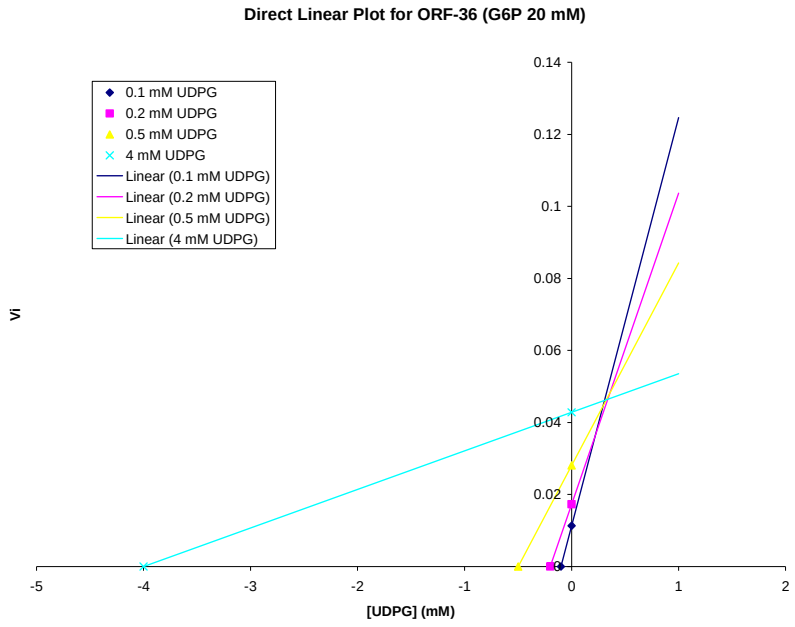

Figure 8: Intersection of the lines indicates the best estimation of K_m and V_{max}.

Table 5 summarizes the k_m and apparent v_{max} values of each G6P concentration using the direct linear plot method.

TABLE 5: K_m and V_{max} values using the Direct Linear Plot

	Apparent K_m (mM)	Apparent V_{max} (s^{-1})
20 mM G6P	0.32	0.046
4 mM G6P	0.43	0.039
1 mM G6P	0.25	0.018
0.5 mM G6P	0.17	0.012

Both methods yielded very similar results, but the direct linear plot gives a better estimation in this case because it is a non-parametric method, meaning that it ignores outliers and gives good results similar to the least squares method when points are reasonable. [12, 13]

Using these apparent k_m and v_{max} values, the actual kinetic constants can then be calculated using *Equation 2*, assuming that the mechanism by which ORF-36 acts is Michaelian (either sequential or ping-pong).

$$V_i = \frac{V_{ab}}{bK_m^A + aK_m^B + K_m K_D + ab} \qquad \textbf{(Eq. 2)}$$

Because this is an iterative process, Mark Ruszczycky allowed the use of his computer program to calculate the kinetic constants. The program was written to weigh more heavily the higher concentrations of UDPG by applying either a constant standard deviation or constant coefficient of variation to minimize error. Based on this, the final steady state kinetic constants for ORF-36 are shown in *Table 6*.

TABLE 6: k_m and v_{max} values of ORF-36

	Constant σ	Constant σ/μ
v_{max}	0.051 ± 0.0023 s^{-1}	0.053 ± 0.0045 s^{-1}
k_m of UDPG	0.36 ± 0.049 mM	0.40 ± 0.057 mM
k_m of G6P	1.5 ± 0.24 mM	1.8 ± 0.28 mM

The kinetic constants of other trehalose phosphate synthases are different than the values reported here. This is most likely attributed to the fact that the experiments done here did not use the real physiological substrate (2SG6P) [14]. Now that a rough estimate of the kinetic parameters and the basic assay protocol has been established, future experiments using the actual substrate can be continued.

Acknowledgments

I would like to thank Dr. Hung-wen Liu for the chance to work in his research lab. Not many undergraduates are blessed with this opportunity. I am indebted to graduate student Eita Sasaki for his guidance, patience, and mentorship that he provided throughout the two years I have been with the group. My thanks also go to Mark Ruszczycky for helping me understanding more about enzyme kinetics. I would also like to thank my family and friends who have supported me throughout my college career.

References

1. Kim, K., Guo, Y., Sulikowski, G.A. 1995. Synthetic Studies of the Angucycline Antibiotics: Stereocontrolled Assembly of the SF 2315B Ring System. *J. Org. Chem.* **60:** 6866–6871

2. Rohr, J. *et al.* 1993. Investigations on the biosynthesis of the angucycline group antibiotics aquayamycin and the urdamycins A and B. Results from the structural analysis of novel blocked mutant products. *J. Org. Chem.* **58:** 2547–2551

3. Trefzer, A. *et al*. 2000. Function of glycosyltransferase genes involved in urdamycin A biosynthesis. *Chemistry and Biology* **7**: 133-142

4. Dharmasiri, N., Dharmasiri, S., Estelle, M. 2005. The F-box protein TIR1 is an auxin receptor. *Nature* **435**: 441-445

5. Settembre E.C., Dorrestein P.C., Zhai H., Chatterjee A., McLafferty F.W., Begley T.P., Ealick S.E. 2004. Thiamin biosynthesis in Bacillus subtilis: structure of the thiazole synthase/sulfur carrier protein complex. *Biochemistry* **43**: 11647-57

6. Pan, Y.T., Carroll, J.D., Elbein, A.D. 2002. Trehalose-phosphate synthase of *Mycobacterium tuberculosis*: Cloning, expression and properties of the recombinant enzyme. *Eur. J. Biochem.* **269:** 6091-6100

7. Cornish-Bowden, A., Eisenthal, R. 1974. The Direct Linear Plot: A New Graphical Procedure for Estimating Enzyme Kinetic Parameters. *Biochem. J.* **139**: 715-720

8. Watanabe, C.H.M., Townsend, C.A., The in Vitro Conversion of Norsolorinic Acid to Aflatoxin B1. An Improved Method of Cell-Free Enzyme Preparation and Stabilization. *J. Am. Chem. Soc.* **120:** 6231-6239

9. Settembre, E.C., *et al.* 2004. Thiamin Biosynthesis in Bacillus subtilis: Structure of the Thiazole Synthase/Sulfur Carrier Protein Complex. *Biochemistry* **43:**11647-11657

10. Yu, M., Magalhaes, M.L.B., Cook, P.F., Blanchard, J.S. 2006. Bisubstrate Inhibition: Theory and Application to N-Acetyltransferases. *Biochemistry* **45:** 14788-14794

11. Storer, A.C., Cornish-Bowden, A. 1974. Applications to the assay of glucokinase with glucose-6-phosphate dehydrogenase as coupling enzyme. *Biochem. J.* **141:** 205-209

12. Cressie, N.A.C., Keightley, D.D. 1979. The underlying structure of the direct linear plot with application to the analysis of hormone-receptor interactions. *Journal of Steroid Biochemistry* **11**: 1173-1180

13. Cornish-Bowden, A., Eisenthal, R. 1974. Statistical considerations in the estimation of enzyme kinetic parameters by the direct linear plot and other methods. *Biochem. J.* **139:** 721–730

14. Vandercammen, A., Francois, J., Hers, H.G. 2004. Characterization of trehalose-6-phosphate synthase and trehalose-6-phosphate phosphatase of Saccharomyces cerevisiae. *European Journal of Biochemistry* **182**: 613-620